

## Photoluminescence and Optical Gain in CuBr Semiconductor Nanocrystals

J. VALENTA<sup>1</sup>) (a), J. DIAN (a), P. GILLIOT (b), and B. HÖNERLAGE (b)

(a) *Department of Chemical Physics and Optics, Faculty of Mathematics and Physics,  
Charles University, Ke Karlovu 3, CZ-121 16 Prague 2, Czech Republic*

(b) *Groupe d'optique nonlinéaire et d'optoélectronique,  
Institut de physique et chimie des matériaux de Strasbourg, UMR 7504 CNRS-ULP,  
23 rue du Loess, F-67037 Strasbourg CEDEX, France*

(Received July 31, 2000; accepted October 2, 2000)

Subject classification: 71.35.-y; 73.21.La; 78.45.+h; 78.55.Hx; 78.67.Bf; S9

Size-dependent excitonic photoluminescence (PL) of CuBr nanocrystals is studied using both, resonant and band-to-band excitation. Narrow excitonic emission lines observed in big nanocrystals (mean radius  $>5$  nm) transform into two wide emission bands in smaller nanocrystals. These two bands are not significantly narrowed under selective excitation within the  $Z_{1,2}$  and  $Z_3$  excitonic absorption bands. Measurements of PL intensity dependence and PL excitation spectra suggest that the emission is due to trapped excitons and biexcitons. Net optical gain of the order of  $10\text{ cm}^{-1}$  from trapped biexcitons can be detected by pump-and-probe transmission measurements as well as amplified spontaneous emission measurements using the variable stripe-length technique.

**1. Introduction** Nanocrystals (NCs) of copper halides embedded in glass matrices are excellent model systems to study excitonic and biexcitonic effects in the weak and intermediate regime of quantum confinement. The most studied material is CuCl, in which biexcitonic emission was observed for the first time in both bulk and nanocrystalline form [1]. The other copper halides (CuBr and CuI) have smaller biexciton binding energies and also their excitonic photoluminescence is much weaker compared to CuCl [2].

The present communication concentrates on the photoluminescence (PL) properties of CuBr NCs in a borosilicate glass. We applied both, resonant and non-resonant laser excitation and the PL-excitation spectroscopy in order to explain the origin of two wide bands typically observed in CuBr PL spectra. Net optical gain was also observed. The results point to the key role of trapped excitons and biexcitons in decay processes.

**2. Samples and Experimental Set-ups** CuBr NCs have been grown in a borosilicate glass matrix using a diffusion controlled process [3]. We study a set of samples made of glass containing CuBr NCs of different mean radius: 9.5, 5.1, 3.9, and 2.8 nm (the mean size of NCs is determined from the spectral position of absorption bands [4]).

The excitation source for PL measurements is either a pulsed nanosecond XeCl-excimer laser ( $\lambda = 308$  nm, pulse duration of 30 ns, repetition rate of about 12 Hz) or a tuneable dye-laser pumped by the excimer laser (spectral width is less than 0.12 meV). In the pump-and-probe transmission measurements we used the spectrally broad super-radiance of a laser-dye solution (excited by a part of the excimer laser output) as probe

---

<sup>1</sup>) Corresponding author; Fax: +420-2-21 91 1249; e-mail: valenta@karlov.mff.cuni.cz

beam (see [4] for details). The PL signal (or probe beam) is dispersed in a single grating 3/4 m monochromator and detected by an optical multichannel analyzer. All experiments are performed at low temperatures using a pumped helium-bath cryostat ( $T = 2$  K) or a continuous flow cryostat.

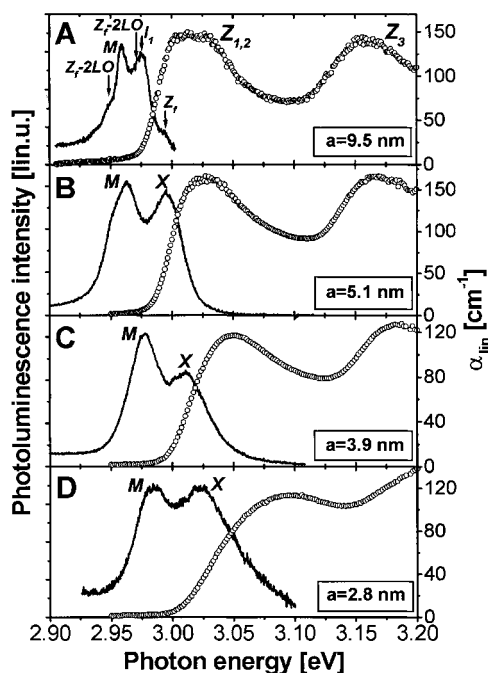
The optical gain was studied by different methods: pump-and-probe transmission measurements, energy transfer, and the variable stripe-length (VSL) method. In the VSL experiment the excitation beam (excimer laser output) was first focused by a cylindrical lens to form a rectangular spot on a slit (with a fixed and a moving jaw) and then projected by a spherical lens on a sample (for the principle of this experiment see e.g. [5]).

### 3. Experimental Results

**3.1 Linear optical properties** The low-temperature (10 K) linear absorption and PL spectra ( $\lambda_{\text{exc}} = 308$  nm, excitation density of about  $60$  kW/cm<sup>2</sup>) of our studied samples are compared in Fig. 1. The low-energy edge of the absorption spectra (dotted curves in Fig. 1) is dominated by the  $Z_{1,2}$  and  $Z_3$  excitonic bands which are significantly blue-shifted with respect to the bulk CuBr due to the quantum confinement effect (Bohr radius of bulk  $Z_{1,2}$  excitons is 1.25 nm, therefore a weak or intermediate regime of quantum confinement takes place in the studied NCs [6]).

The PL spectrum of the sample containing big NCs (Fig. 1A, solid line) resembles a spectrum of bulk CuBr crystals [2] and is labelled accordingly. The  $Z_t$ ,  $Z_t - \text{LO}$ , and  $Z_t - 2\text{LO}$  peaks are attributed to the lowest triplet exciton recombination and its phonon replicas. The  $I_1$  and  $M$  peaks are due to excitons bound to impurities and biexciton (free or bound) recombination, respectively. PL spectra of samples with a mean size

of NCs of about 5 nm and smaller (Fig. 1B–D) have only two broad emission bands (labelled  $M$  and  $X$ ) which are the main subject of this paper.



**3.2 PL vs. excitation intensity and wavelength** The  $X$  and  $M$  emission bands have significantly different intensity dependences. The  $X$ -band intensity increases linearly with the excitation intensity while the  $M$ -band shows superlinear

Fig. 1. Linear excitonic absorption (dotted curves) and photoluminescence spectra (solid lines) of samples containing CuBr NCs with a mean radius of (A) 9.5, (B) 5.1, (C) 3.9, and (D) 2.8 nm ( $T \approx 10$  K). PL is excited by the XeCl laser (308 nm, about  $60$  kW/cm<sup>2</sup>). For the meaning of the labels of spectral lines see Section 3.1

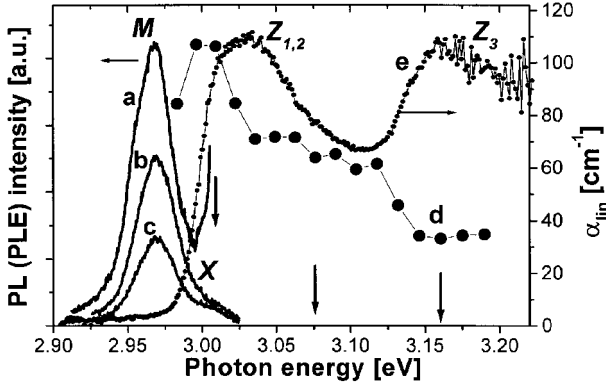


Fig. 2. Selectively excited photoluminescence ( $\lambda_{exc} = 308$  nm, sample with CuBr NCs of  $a = 5.1$  nm at  $T = 10$  K). The curves (a)–(c) on the left-hand side (bold lines) are PL spectra excited resonantly with excitonic absorption at (a) 3.009, (b) 3.076, and (c) 3.16 eV, respectively (the spectral position of laser excitation is indicated by arrows). The PL excitation spectrum (d) for emission detected at 2.97 eV is represented by large dots. A linear absorption spectrum of the sample (e, small dots) is shown for comparison

increase ( $I_{PL}^M \sim I_{exc}^x$ , where  $x$  is between 1.4 and 1.8). This observation agrees well with the PL measurements on CuCl [1] and CuBr [7] NCs.

Resonant excitation through the  $Z_{1,2}$  and  $Z_3$  excitonic absorption bands produces mainly M-band emission (Fig. 2, curves a–c). The relative intensity of the X-band is highly suppressed when compared to band-to-band excitation (Fig. 1B). It is important to note that the widths of emission spectra are not significantly reduced through the resonant excitation. This fact is in contrast to the selective narrow absorption changes (transient and persistent spectral-holes) which are produced in our samples by the same resonant excitation at low temperatures (see [8] for details). The PL excitation spectrum for the detection at the center of the M-band (2.969 eV) is shown by large dots in Fig. 2 (curve d). The maximum of excitation efficiency lies below the maximum of the  $Z_{1,2}$  band, roughly at the position of the X-band.

**3.3 Optical gain** In spite of the relatively low intensity of PL detected in our CuBr NCs, we tried to achieve stimulated emission from our samples. Indeed, it was possible to observe small net optical gain up to  $10 \text{ cm}^{-1}$  by both the pump-and-probe and the VSL amplified spontaneous emission (ASE) measurements.

When pumping with an excimer laser (308 nm), transient changes in absorption spectrum are observed. They roughly correspond to the small blue shift of the whole excitonic absorption bands [4] with one important feature – reduced absorption on the low-energy edge of the  $Z_{1,2}$  band. Figure 3A shows the edge of the linear absorption spectrum compared to the differential absorption produced by the pumping at 308 nm ( $150 \text{ kW/cm}^2$ ,  $T \approx 20$  K). The decrease of absorption overcomes linear absorption between 2.94 and 3 eV (dashed area in Fig. 3A). The corresponding optical gain reaches  $10 \text{ cm}^{-1}$  at its maximum.

The ASE measurement is performed by excitation of a narrow stripe of variable length on the edge of a sample. (To some extent, the VSL method is equivalent to the pump-and-probe experiment, the spontaneous emission playing the role of a probe.) The detected PL intensity  $I_T$  dependence on the stripe length  $l$  is described by the equation [5]

$$I_T(l, \lambda) \sim I_{sp}(\lambda) \frac{\exp[G(\lambda) l] - 1}{G(\lambda) l},$$

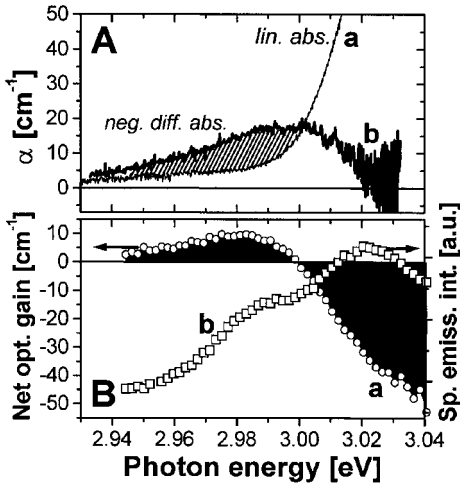


Fig. 3. Optical gain measurements (CuBr NCs 3.9 nm,  $T \approx 15\text{--}20$  K). A) Linear absorption at the long-wavelength edge of the  $Z_{1,2}$  band (a) compared with the inverse differential absorption (b) produced by band-to-band excitation at 308 nm ( $150 \text{ kW/cm}^2$ ). The difference between curves (a) and (b) (dashed area) indicates a net optical gain. B) Net optical gain spectrum (a – black area with circles) and spectrum of spontaneous PL emission (b – white squares) calculated from the amplified spontaneous emission measured by the VSL method. Excitation by XeCl laser at 308 nm,  $110 \text{ kW/cm}^2$

where  $I_{\text{sp}}$  and  $G$  are spontaneous emission intensity (per unit area of excited surface) and effective optical gain/loss (absorption), respectively. The  $I_{\text{sp}}(\lambda)$  and  $G(\lambda)$  spectra can be extracted from  $I_{\text{T}}(l, \lambda)$  by fitting the  $I_{\text{T}}$  dependence on  $l$  for each wavelength  $\lambda$ . Figure 3B shows such calculated spectra of gain (curve a) and spontaneous emission (curve b) for excitation density of  $110 \text{ kW/cm}^2$  ( $T \approx 15$  K). Again, net optical gain is observed at the position of the M band. Compared with biexcitonic optical gain of about  $200 \text{ cm}^{-1}$  measured by Masumoto and co-workers for CuCl NCs in NaCl matrix [9] maximal gain in CuBr NCs is more than one order of magnitude smaller, but it is comparable to values obtained for CuCl NCs in glass [10].

**4. Discussion** Taking into account all experimental observations we propose that the X- and M-bands are due to *radiative recombination of trapped excitons and trapped biexcitons*, respectively. The band-to-band excitation creates excitons inside CuBr NCs, which can form biexcitons if the generation rate is high enough. The resonant excitation of the  $Z_{1,2}$  excitonic state is even more efficient, so creation of a second exciton in a NC before recombination of the first (trapped) exciton is more probable. For photon energy equal to half of the biexciton energy, direct two-photon excitation of biexcitons can take place. This phenomenon is a probable origin of the PLE maximum (Fig. 2, curve d) lying below the  $Z_{1,2}$  band. We suppose that the majority of the generated excitons and biexcitons becomes localized at the surface of a NC (the surface polarization effect should be considered [11]) and then they recombine back or dissociate. There is probably a relatively wide distribution of trap states even in NCs of uniform size, which causes an omnipresent wide shape of PL bands (Fig. 2, curves a–c). (We note that the localization and trapping of biexcitons was recently observed in CuCl nanocrystals [12] and in narrow quantum wells and semiconductor alloys – see for example [13].)

The observed moderate optical gain is probably due to stimulated emission between biexciton and exciton states. An alternative explanation could be exciton–exciton scattering [14] (it was observed recently in thin CuBr films [15]). More data are neces-

sary to understand the gain mechanism and the effect of permanent PL degradation on it [16].

In summary, we have studied photoluminescence and optical gain in CuBr nanocrystals in a glass matrix. Nanocrystals with mean radii of about 5 nm and smaller show two broad emission bands that are attributed to the recombination of trapped excitons and trapped biexcitons.

**Acknowledgements** We would like to thank Prof. A.I. Ekimov (Ioffe Physico-Technical Institute, St. Petersburg) for the high quality samples. This work was supported in part by the grants No. B1112901 from GAAV CR and No. 202/98/0669 from GACR. J.V. has received the financial support from the French Government (MENRT – “Réseau de formation–recherche, Europe centrale et orientale”) which is gratefully acknowledged.

## References

- [1] R. LÉVY, L. MAGER, P. GILLIOT, and B. HÖNERLAGE, *Phys. Rev. B* **44**, 11286 (1991)
- [2] M. UETA, H. KANZAKI, K. KOBAYASHI, Y. TOYOZAWA, and E. HANAMURA, *Excitonic Processes in Solids*, Springer-Verlag, Berlin 1984 (Chap. 3).
- [3] A.I. EKIMOV, A.I. EFROS, M.G. IVANOV, and A.A. ONDUSCHENKO, *Solid State Commun.* **56**, 921 (1985).
- [4] J. VALENTA, J. MONIATTE, P. GILLIOT, B. HÖNERLAGE, J.B. GRUN, R. LEVY, and A.I. EKIMOV, *Phys. Rev. B* **57**, 1774 (1998).
- [5] K.L. SHAKLEE and R.F. LEHENY, *Appl. Phys. Lett.* **18**, 475 (1971).
- [6] L. BANYAI and S.W. KOCH, *Semiconductor Quantum Dots*, World Scientific, Singapore 1993.
- [7] U. WOGGON, O. WIND, W. LANGBEIN, D. GOGOLIN, and C. KLINGSHIRN, *J. Lumin.* **59**, 135 (1994).
- [8] J. VALENTA, J. DIAN, J. HÁLA, P. GILLIOT, and R. LÉVY, *J. Chem. Phys.* **111**, 9398 (1999).
- [9] Y. MASUMOTO, T. KAWAMURA, and K. ERA, *Appl. Phys. Lett.* **62**, 225 (1993).
- [10] P. FALLER, B. KIPPELEN, B. HÖNERLAGE, and R. LÉVY, *Opt. Mater.* **2**, 39 (1993).
- [11] L. BANYAI, P. GILLIOT, Y.Z. HU, and S.W. KOCH, *Phys. Rev. B* **24**, 14136 (1992).
- [12] S. YANO, T. GOTO, T. ITOH, and A. KASUYA, *Phys. Rev. B* **55**, 1667 (1997).
- [13] W. LANGBEIN and J.M. HVAM, *phys. stat. sol. (b)* **206**, 111 (1998).
- [14] C. KLINGSHIRN and H. HAUG, *Phys. Rep.* **70**, 315 (1981).
- [15] H. ICHIDA, M. NAKAYAMA, and H. NISHIMURA, *J. Lumin.* **87–89**, 235 (2000).
- [16] J. VALENTA, J. DIAN, P. GILLIOT, and R. LEVY, *J. Lumin.* **86**, 341 (2000).

